Journal of Materials Chemistry B

PAPER

View Article Online
View Journal | View Issue

Cite this: J. Mater. Chem. B, 2014, 2, 2008

Received 26th September 2013
Accepted 23rd January 2014

DOI: 10.1039/c3tb21339k

www.rsc.org/MaterialsB

A selective NIR-emitting zinc sensor by using Schiff base binding to turn-on excited-state intramolecular proton transfer†

Junfeng Wang,[a] Yingbo Li,[c] Ernest Duah,[a] Sailaja Paruchuri,[a] Demin Zhou[c] and Yi Pang*[ab]

A rational design has led to a highly selective and cell-permeable zinc sensor, which exhibits *not only* a large fluorescence turn-on at ~545 nm *but also* the desirable NIR emission (~720 nm) with a large Stokes' shift, providing a practical sensor platform with two emission channels for reliable zinc detection.

Significant interest exists to detect and quantify the dynamic zinc ion flux in live tissues or animals, as zinc is an essential element which plays important roles in many cellular processes including gene expression and signal transduction.[1] For *in vivo* applications,[2] the molecular probe is required to emit optical signals in the near infrared (NIR) region (700–900 nm), as NIR light can penetrate more deeply into biological tissues.[3] Although many zinc probes are available,[4] few can give NIR emission,[5,6] and most are based on cyanine dyes. The cyanine dyes, however, exhibit a small Stokes' shift (typically about 20–50 nm), which hampers their broad applications. For example, a cyanine-based zinc sensor has a 730 nm excitation wavelength and a 780 nm emission wavelength.[5] It remains a challenge to develop a Zn^{2+} sensor that exhibits *not only* desirable NIR emission, *but also* large Stokes' shift and high selectivity (*e.g.* without interference from the structurally similar Cd^{2+} cations).

2-(2′-Hydroxyphenyl)benzoxazole (HBO) **1** has emerged to be an interesting component in the sensor design,[7,8] as it can undergo the excited-state intramolecular proton transfer (ESIPT) to produce the emission with a large Stokes' shift (*ca.* 150–200 nm). Among the few HBO derivatives for zinc detection, O'Halloran's group reported **1a** for intracellular Zn^{2+} sensing, *via* formation of zinc complex **1a-Zn** (λ_{max} = 376 nm, λ_{em} = 443 nm).[7] Kwon and co-workers reported another HBO derivative **1b** (λ_{max} = 379 nm, λ_{em} = 550 nm), whose zinc complex **1b-Zn** gives enhanced emission (λ_{max} = 443 nm, λ_{em} = 542 nm).[9] Formation of zinc complex **1-Zn**, however, removes the phenolic proton in HBO, thereby disabling the ESIPT mechanism and diminishing the Stokes' shift.

Recently, our group has designed the bis(HBO) **3-Zn**, by changing the R_1 and R_2 substituents in **1-Zn** to respective benzoxazole and hydroxy groups to introduce the 2nd HBO.[10–12] Upon binding to Zn^{2+} cations, the weak fluorescence of **3** is turned on, giving both green (λ_{em} ≈ 540 nm) and NIR emission (λ_{em} ≈ 750 nm). The NIR turn-on signal from **3**, however, also responds to Cd^{2+} cations.[11] It remains a challenge to develop a Zn^{2+} sensor that gives desirable NIR emission without interference from the structurally similar Cd^{2+} cations. In addition, the intensity of the desirable NIR emission from **3-Zn** also needs to be further tuned. And the synthesis of the sensor needs to be simplified for practical applications.

In an effort to tune the performance of the ESIPT probe, the complex **4-Zn** appears to be an interesting system. In comparison with **3-Zn**, the complex **4-Zn** uses an isolated imine bond (–CH=N–) to bind Zn^{2+} cations. When the zinc-binding benzoxazole fragment in **3** is replaced by a –CH=N– bond, one of the two HBO units in bi(HBO) **3** is removed, which could influence the ESIPT signal of the neutral ligand and its metal complexes. In addition, the zinc-chelation of **4** will form a more stable five-membered ring "A" involving the –CH=N– and pyridyl groups, in contrast to a six-membered ring in **3-Zn** that involves the benzoxazole and pyridyl groups. Such structural change could perturb the interaction between the zinc cation and phenolic oxygen, thereby tuning the ESIPT of the 2nd HBO unit.

While some Schiff-base chemosensors are known for selective Zn^{2+} detection,[13–17] they give fluorescence either in the blue[14,16,17] or green colors[13,15] with small Stokes' shift (~30 nm). In addition, the known Schiff-base sensors are dependent on the fluorescence turn-on through metal binding-induced isomerization[13] of the –C=N– bond with little spectral shift. Reasoning that using a Schiff base ligand could improve the selectivity in Zn^{2+} binding, we decided to explore the *mono* HBO

[a]*Department of Chemistry, The University of Akron, Akron, Ohio 44325, USA. E-mail: yp5@Uakron.edu*

[b]*Maurice Morton Institute of Polymer Science, The University of Akron, Akron, Ohio 44325, USA*

[c]*State Key Laboratory of Natural and Biomimetic Drugs, School of Pharmaceutical Sciences, Peking University, Beijing 100191, China*

† Electronic supplementary information (ESI) available. See DOI: 10.1039/c3tb21339k

sensor **4**. Intriguingly, the sensor **4** exhibited great selectivity toward Zn^{2+} binding, which turns on the ESIPT to give the desirable NIR emission (at ~720 nm) with a large Stokes' shift (~260 nm). The findings demonstrate that a Schiff base can serve as an effective switch for the ESIPT turn-on, whose excellent selectivity to bind zinc cations makes the NIR sensor an attractive candidate for practical applications.

Synthesis of **4** was accomplished by reaction of 2-hydrozinylpyridine with the corresponding aldehyde **6** in high yield (Scheme 2). The simplicity in the synthesis of the ligand **4** was in sharp contrast to that of ligand **3** which used a sequence of four synthetic steps from the aldehyde (with low yield).[12] The binding properties of **4** to Zn^{2+} cations were examined in EtOH/HEPES (Fig. 1). As the Zn^{2+} cations were added, a new absorption band was generated at about 450 nm. The new band was attributed to the removal of a phenolic proton as shown in the **4-Zn** complex. The signal change appeared to be complete when one equivalent Zn^{2+} was added, suggesting a 1 : 1 ligand-to-metal ratio (ESI Fig. S3†). Addition of other cations, such as Al^{3+}, however, did not cause a notable bathochromic shift, indicating that their bindings were not sufficiently strong to remove the phenolic proton (Fig. 1, S5 and S6†). The sensor also showed weak binding to Cd^{2+} cations (Fig. 1).

The ligand **4** gave a weak fluoresence peak at 580 nm (ϕ_{fl} = 0.05). Upon addition of Zn^{2+} cations, the fluorescence significantly increased (ϕ_{fl} = 0.26 in 1 : 1 EtOH/H_2O), giving two new emission peaks at 545 and ~720 nm (Fig. 2a and S2†, and Table 1), which correspond to the emission from the *enol* and *keto* tautomers of **4-Zn**, respectively. NIR emission was relatively stronger in pure methanol (ESI Fig. S4†). The green fluorescence turn-on could be easily observed, making it also useful for naked eye detection (Fig. 2b). Interestingly, addition of other cations (K^+, Na^+, Ag^+, Cd^{2+}, Ca^{2+}, Mg^{2+}, Pb^{2+}, Ni^{2+}, Hg^{2+}, Co^{2+}, Cu^{2+}, Cr^{3+}, Fe^{3+}, Al^{3+}) to **4** did not induce the dual emissions at 545 and 720 nm. In other words, the probe molecule **4** is silent to Cd^{2+} cations, as its binding could not remove the phenolic proton (a necessary step to simultaneously shift the emission and turn on the ESIPT for NIR emission). The Al^{3+} cations only induced an enhanced emission at ~610 nm, as its stronger Lewis acid character could lead to a moderately strong interaction with the phenol segment (Fig. S6†). In summary, the sensor **4** displayed an excellent selectivity toward Zn^{2+} binding,

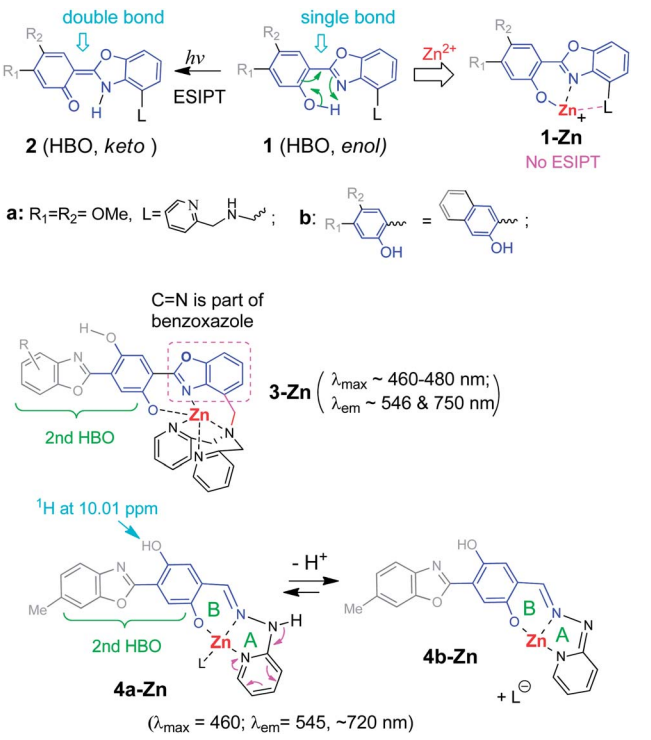

Scheme 1 Structures of 2-(2′-hydroxyphenyl) benzoxazole (HBO) derivatives, where the original HBO unit is shown in blue.

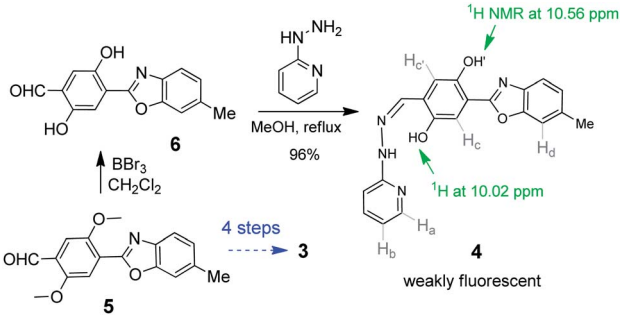

Scheme 2 Synthesis of sensor **4**.

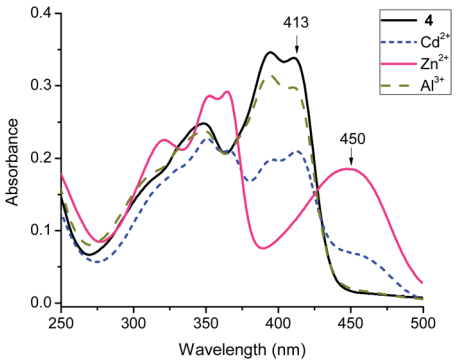

Fig. 1 Absorbance spectra of **4** (10 μM) in EtOH/HEPES (10 mM) (1 : 1) (pH = 7.2), upon addition of 5 equiv. of different cations.

Table 1 Absorption and emission of ESIPT sensors

	Absorption λ_{max} (nm)	Emission λ_{em} (nm)	Stokes' shift
1a	337	407	5103 cm^{-1} (70 nm)
1a-Zn	376	443	4022 cm^{-1} (67 nm)
1b	379	550	8203 cm^{-1} (171 nm)
1b-Zn	443	542	4123 cm^{-1} (99 nm)
3	412	456, 610[a,11]	7878 cm^{-1} (198 nm)
3-Zn	465	546, 750[a]	8172 cm^{-1} (285 nm)
4	413	580	6971 cm^{-1} (167 nm)
4-Zn	450	545, 720[a]	8333 cm^{-1} (270 nm)

[a] Indicates the peak used to calculate Stokes' shift.

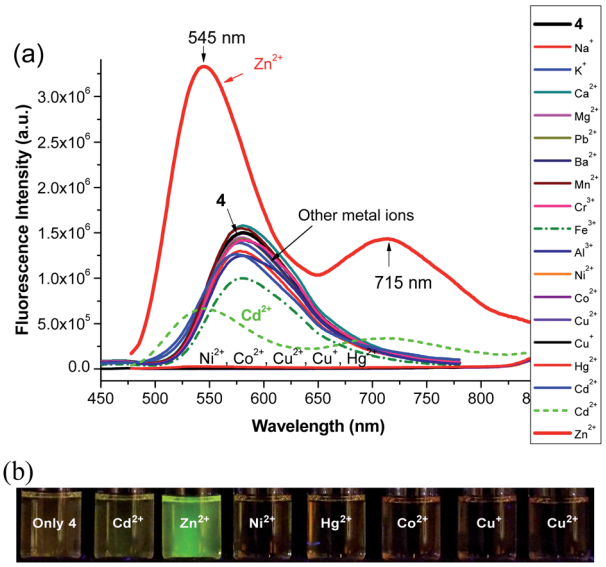

Fig. 2 (a) Fluorescence spectra of **4** (10 μM) in EtOH : HEPES = 1 : 1 (pH = 7.2) upon addition of 5 equiv. of different ions. (b) Fluorescence images after addition of different metal ions to **4** (10 μM in EtOH : HEPES = 1 : 1).

which simultaneously induced both fluorescence turn-on and a large spectral shift.

In the ^{1}H NMR of ligand **4** (Fig. 3), the signals at 10.56 and 10.02 ppm were attributed to the phenolic protons (−OH′ and –OH, respectively),[18] while the signals at 11.09 ppm were assigned to the amine.[19] Upon addition of Zn^{2+} (one equiv.), the –OH′ at 10.56 ppm was transformed to –OH″ (at ~10 ppm), as a consequence of forming **4-Zn**. The unusually broad signals at ~10 ppm, when 0.2–0.5 equiv. of Zn^{2+} was added, were partially attributed to the presence of both –OH (in **4**) and –OH" (in **4-Zn**). Two singlet Ar−H signals (H_c or $H_{c'}$ at 7.38, and H_d at 7.44 ppm) were gradually decreased with addition of Zn^{2+}, in agreement with the large electronic impact associated with the formation of the metal complex. It should be noted that the

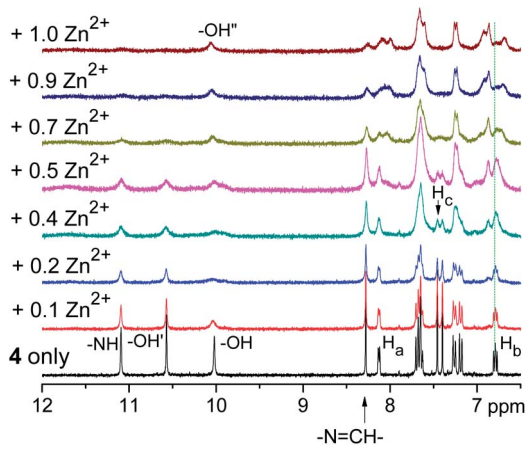

Fig. 3 ^{1}H NMR titration of **4** with $Zn(OAc)_2$ in DMSO-d_6; disappearance of signal H_c at ~7.38 ppm supports the 1 : 1 ligand-to-metal ratio.

2-(hydrozino)pyridine[20] unit in **4a-Zn** can be tautomerized to give **4b-Zn** (Scheme 1), which might also contribute to the signal broadening from the ^{1}H NMR. Mass spectrometry detected m/z = 422.0496 by HRMS (Fig. 4), corresponding to [**4b-Zn** − L] (calcd for $C_{20}H_{14}N_4O_3Zn$: 422.0357, see ESI Fig. S14†).

In order to clarify the interactions of **4** with different metal ions, the UV-vis absorption and fluorescence spectra of **4** (10 μM in EtOH : H_2O = 1 : 1 solutions) were studied by addition of 5 equiv. of different cations (ESI Fig. S5 and S6†). In addition to no response to physiologically important K^+, Na^+, Ca^{2+} ions, the sensor also exhibited no observable fluorescence response to Cd^{2+} cations, which led to greatly improved selectivity over the previous sensor **3**.[9,10] While some cations (Ag^+, Co^{2+}, Ni^{2+} and Cu^{2+}) quenched the fluorescence, addition of Cr^{3+}, Fe^{3+} and Al^{3+} cations slightly increased the fluorescence whose signals were red-shifted by ~25–37 nm. Only Zn^{2+} binding gave enhanced emissions at 545 nm and ~720 nm, which are significantly shifted from the neutral ligand (580 nm) to allow the positive identification of the zinc cations.

As revealed from Fig. 2, only zinc binding to **4** could effectively turn on the ESIPT, giving enhanced emission from both *enol* ($\lambda_{em} \approx 545$ nm) and *keto* tautomers ($\lambda_{em} \approx 720$ nm). A peculiar question is why the ligand **4** can bind Zn^{2+} cations well, while being silent to the Cd^{2+} cations with similar atomic configuration ([Ar]$3d^{10}$ for Zn^{2+} and [Kr]$4d^{10}$ for Cd^{2+}).[21] On the basis of quick disappearance of the –OH signal at ~10 ppm (^{1}H NMR in Fig. 3), the initial step might involve a weak interaction of a metal cation with the imine –CH=N-, forming intermediate **5**. Interaction with the pyridyl then led to a more stable 5-membered ring "A" as shown in **6**. The Zn^{2+} cation in **6a** could further interact with the adjacent hydroxyl group to form the fused 6-membered ring "B", which requires twisting of the "HBO" fragment from the Schiff base fragment (ring A). The intermediate **7** could quickly lose a proton to give **4-Zn**, which is detected in the absorption spectrum. From the fluorescence titration data, the association constant was determined to be $K_a = 2.28 \times 10^5$ M^{-1}.

When Cd^{2+} was used, the interaction pattern appeared to be quite different. The ^{1}H NMR titration using Cd^{2+} revealed that the pyridyl protons H_a and H_b were not affected after addition of one equiv. of Cd^{2+} cations (ESI Fig. S12†), indicating the lack of tight and stable binding to the pyridyl ring. Therefore, the equilibrium between **6b** and **8** might occur without forming the fused rings A–B in **4-Cd**. This might be due to the larger size of

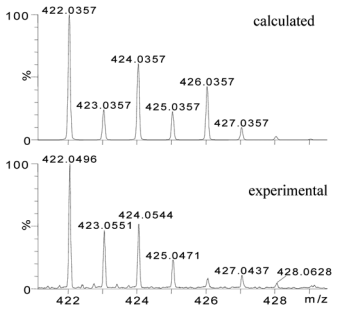

Fig. 4 Mass spectrum of **4-Zn** (calcd for $C_{20}H_{14}N_4O_3Zn$: 422.0357).

the Cd^{2+} cation (or longer Cd–N & Cd–O bonds), which destabilizes the fused A–B rings in **4-Cd** as observed from a molecular modeling comparison (ESI Fig. S11†). The proposed fast equilibrium between **6b** and **8** accounts for the experimental findings: (a) addition of Cd^{2+} cations induced a smaller peak of bathochromic shift in the absorption spectrum of **4** (Fig. 1), indicating the weak binding of Cd^{2+} cations to phenol (without removing phenolic protons) and (b) disappearance of phenolic protons in ^{1}H NMR (ESI Fig. S12†). Although the strength of lewis acid ($Zn^{2+} > Cd^{2+}$) could play a role in their differentiation, Lewis acidity alone could not explain the lack of formation of **4-Cd** under the experimental conditions (Scheme 3).

In the zinc-sensing process, an intriguing question is how the zinc-binding in **4-Zn** could affect the ESIPT event in HBO, in comparison with the ligand **4**. As shown in **1** → **2** (Scheme 1), the ESIPT event in HBO is dependent on the electronic connection between the phenol and benzoxazole fragments. Computation with DFT at the B3LYP/6-31 G level revealed that the LUMO of HBO in **4** had a large orbital interaction between the phenol and benzoxazole fragments (Fig. 5), which could facilitate the proton transfer in the excited state. The calculation was consistent with the experimental finding that the ligand **4** gave only ESIPT emission, indicating the important role of the electronic connection in the LUMO of HBO. The calculation further revealed that the electronic connection between the phenol and benzoxazole fragments became weaker in the LUMO of **4-Zn**, which might be responsible for partial conversion of the excited **4-Zn** (the *enol* tautomer) to its *keto* tautomer. This led to emission from both *enol* and *keto* tautomers of **4-Zn**. In other words, the new zinc sensor exhibited several attractive features: (1) using Schiff base binding to weaken ESIPT emission to reduce the background emission signal; Lack of *enol* emission from **4** is also an improved feature over the previous sensor **3**;[11] (2) introducing zinc binding to induce a large spectral shift for emission in the NIR region; and (3) using zinc binding to perturb the electronic linkage to attenuate the ESIPT, thereby allowing dual emission.

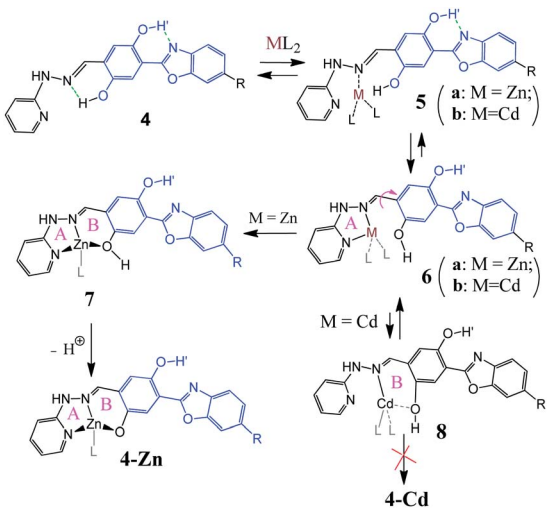

Scheme 3 Possible formation of Zn^{2+} and Cd^{2+} complexes.

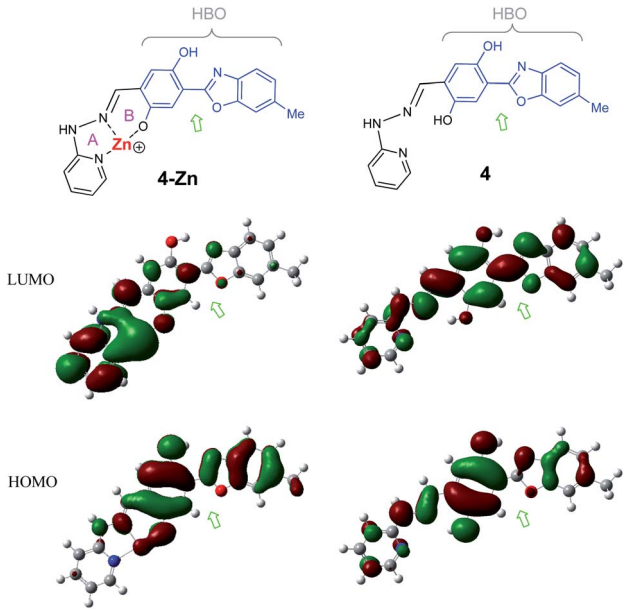

Fig. 5 The HOMO and LUMO orbitals of **4-Zn** and **4**, calculated with DFT at the B3LYP/6-31 G level using Gaussian 09. The double arrows indicate the orbital lobes between the phenol and benzoxazole fragments.

To illustrate the potential biological application, sensor **4** was applied to visualize intracellular Zn^{2+} in both human cancer cells (HepG2) and human umbilical vein endothelial cells (HUVECs) (see Fig. 6, and ESI Fig. S13† for more details). For this purpose, cells were first incubated with 30 μM of Zn^{2+} for 30 min and then further treated with 10 μM dye **4** for another 30 min before imaging. While very weak fluorescence was observed in cells treated with only dye **4** (Fig. 6b), strong

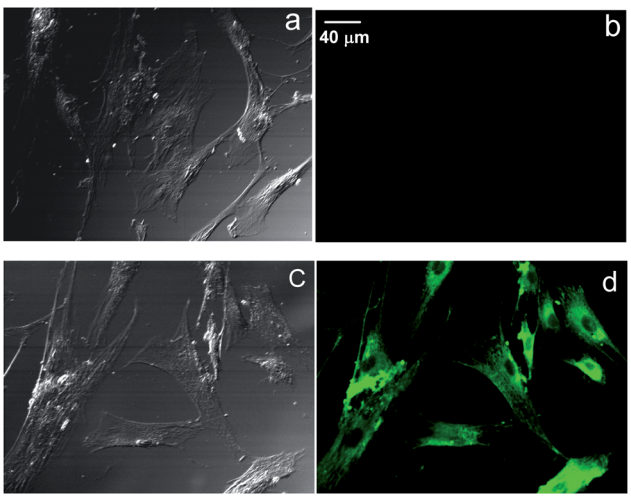

Fig. 6 Confocal fluorescence images of human mesenchymal stem cells (hMSCs) excited with a 488 laser. The images were collected at bright field (a and c) and green channel (535–565 nm; b and d) on an Olympus FV1000-Filter confocal microscope. a → b: the cells were incubated with dye **4** for 60 min at 37 °C; c → d: the cells were first treated with $Zn(OAc)_2$ (30 μM) for 30 min and further exposed to dye **4** (10 μM) for another 60 min at 37 °C.

fluorescence was observed from both cell lines which are treated with both Zn^{2+} and dye **4** (Fig. 6d and S13c†). These results demonstrate that the probe is permeable to cells, binds to intracellular Zn^{2+}, and emits strong fluorescent light upon binding to the metal ion, and thus is highly suitable for determining intracellular Zn^{2+}.

In conclusion, we have demonstrated a cell permeable sensor which is highly selective (almost *specific*) for zinc cations. The sensor design successfully utilizes the Schiff base in the zinc-binding event, which subsequently induces the ESIPT of HBO **4** to produce a large fluorescence response. In contrast to the existing sensors that typically give one signal, the new sensor generates *not only* a large fluorescence turn-on at ~545 nm *but also* the desirable NIR emission (~720 nm) with a large Stokes' shift. Since *only* the zinc binding can induce the ESIPT, the sensor can be used for reliable monitoring of Zn^{2+} concentration. The metal binding studies also reveal that the *specific* zinc response could be attributed to the sensor's ability to form the fused A–B rings with Zn^{2+} (as shown in **4-Zn**). The strict binding requirement associated with the fused A–B rings makes the sensor silent to Cd^{2+}, whose interference often poses a challenge in Zn^{2+} detection. This could be due to the combination of the following reasons: (1) weak binding of Cd^{2+} to **4** (Fig. 1), as cation's relative large size destabilizes the fused A–B rings and (2) fluorescence quenching minimizes its interference (Fig. 2).

Acknowledgements

This work was supported by National Institute of Health (Grant no: 1R15EB014546-01A1). We also thank the Coleman endowment from the University of Akron for partial support.

Notes and references

1 E. L. Que, D. W. Domaille and C. J. Chang, *Chem. Rev.*, 2008, **108**, 1517–1549.
2 R. Weissleder and V. Ntziachristos, *Nat. Med.*, 2003, **9**, 123.
3 J. L. Kovar, M. A. Simpson, A. Schutz-Geschwender and D. M. Olive, *Anal. Biochem.*, 2007, **367**, 1.
4 P. Carol, S. Sreejith and A. Ajayaghosh, *Chem. – Asian J.*, 2007, **2**, 338–348.
5 B. Tang, H. Huang, K. Xu, L. Tong, G. Yang, X. Liu and L. An, *Chem. Commun.*, 2006, 3609–3611.
6 K. Kiyose, H. Kojima, Y. Urano and T. Nagano, *J. Am. Chem. Soc.*, 2006, **128**, 6548–6549.
7 M. Taki, J. L. Wolford and T. V. O'Halloran, *J. Am. Chem. Soc.*, 2004, **126**, 712.
8 J. Wu, W. Liu, J. Ge, H. Zhang and P. Wang, *Chem. Soc. Rev.*, 2011, **40**, 3483.
9 J. E. Kwon, S. Lee, Y. You, K. H. Baek, K. Ohkubo, J. Cho, S. Fukuzumi, I. Shin, S. Y. Park and W. Nam, *Inorg. Chem.*, 2012, **51**, 8760.
10 Y. Xu and Y. Pang, *Chem. Commun.*, 2010, **46**, 4070.
11 Y. Xu and Y. Pang, *Dalton Trans.*, 2011, **40**, 1503.
12 Y. Xu, Q. Liu, B. Dou, B. Wright, J. Wang and Y. Pang, *Adv. Healthcare Mater.*, 2012, **1**, 485.
13 J. S. Wu, W. M. Liu, X. Q. Zhuang, F. Wang, P. F. Wang, S. L. Tao, X. H. Zhang, S. K. Wu and S. T. Lee, *Org. Lett.*, 2007, **9**, 33.
14 L. Li, Y.-Q. Dang, H.-W. Li, B. Wang and Y. Wu, *Tetrahedron Lett.*, 2010, **51**, 618.
15 L. Wang, W. Qin and W. A. Liu, *Inorg. Chem. Commun.*, 2010, **13**, 1122.
16 W. H. Hsieh, C.-F. Wan, D.-J. Liao and A.-T. Wu, *Tetrahedron Lett.*, 2012, **53**, 5848.
17 H.-Y. Lin, P.-Y. Cheng, C.-F. Wan and A.-T. Wu, *Analyst*, 2012, **137**, 4415.
18 The proton signal at 10.02 ppm is assigned to –OH near the benzoxazole ring, with the aid of compound **6**.
19 A. R. Todeschini, A. L. de Miranda, K. C. da Silva, S. C. Parrini and E. J. Barreiro, *Eur. J. Med. Chem.*, 1998, **33**, 189.
20 D. C. Oniciu, I. Ghivirga, A. R. Katritzky, P. J. Steel and P. Tomasik, *Chem. Heterocycl. Compd.*, 2001, **37**, 723–726.
21 Atomic radii of the elements, *CRC Handbook of Chemistry and Physicis*, ed. D. R. Lide, CRC Press, Boca Raton, 90th edn, 2009, pp. 9–49.

